Conf-901007--49

Rec'd OSTI

JAN 2 2 1991

PAPER

CONF-901007--49

DE91 006496

U.S.-ITER ACTIVATION ANALYSIS*

H. Attaya, Y. Gohar, and D. Smith
Argonne National Laboratory
Argonne, IL USA

DISCLAIMER

This report was prepared as an account of work sponsored by an agency of the United States Government. Neither the United States Government nor any agency thereof, nor any of their employees, makes any warranty, express or implied, or assumes any legal liability or responsibility for the accuracy, completeness, or usefulness of any information, apparatus, product, or process disclosed, or represents that its use would not infringe privately owned rights. Reference herein to any specific commercial product, process, or service by trade name, trademark, manufacturer, or otherwise does not necessarily constitute or imply its endorsement, recommendation, or favoring by the United States Government or any agency thereof. The views and opinions of authors expressed herein do not necessarily state or reflect those of the United States Government or any agency thereof.

The submitted manuscript has been authored by a contractor of the U. S. Government under contract No. W-31-109-ENG-38. Accordingly, the U. S. Government retains a nonexclusive, royalty-free license to publish or reproduce the published form of this contribution, or allow others to do so, for U. S. Government purposes.

September 1990

MASTER

* Work supported by the Office of Fusion Energy, U.S. Department of Energy under Contract Number W-31-109-Eng-38.

Paper to be presented at the 9th Topical Meeting on The Technology of Fusion Energy, Oak Brook, IL, October 7-11, 1990.

DISTRIBUTION OF THIS DOCUMENT IS UNLIMITED

US-ITER ACTIVATION ANALYSIS*

H. Attaya, Y. Gohar, and D. Smith
Argonne National Laboratory
Argonne, IL 60439-4832
(708) 972-4484

ABSTRACT

Activation analysis has been made for the US ITER design. The radioactivity and the decay heat have been calculated, during operation and after shutdown for the two ITER phases, the Physics Phase and the Technology Phase. The Physics Phase operates about 24 full power days (FPDs) at fusion power level of 1100 MW and the Technology Phase has 860 MW fusion power and operates for about 1360 FPDs. The point-wise gamma sources have been calculated everywhere in the reactor at several times after shutdown of the two phases and are then used to calculate the biological dose everywhere in the reactor. Activation calculations have been made also for ITER divertor. The results are presented for different continuous operation times and for only one pulse. The effect of the pulsed operation on the radioactivity is analyzed.

INTRODUCTION

The International Thermonuclear Experimental Reactor (ITER) is a collaborative effort among the USA, USSR, Japan, and the European Community. ITER is a tokamak device that is designed to demonstrate the controlled ignition with extended burn in D-T plasma, with steady state as an ultimate goal, and the performance of the required fusion reactor technologies. These two major objectives are achieved through the operation of ITER in two phases, a Physics Phase which will focus on physics experiments as well as the demonstration of integrated fusion technology, and a Technology Phase which will be devoted to technology testing.

The Physics Phase will last for six years and will utilize different plasmas. In the first four years of this phase, H, D, and D-He3 plasmas will be used, and in the last two years, the D-T plasma will be utilized. The expected first wall fluence at the end of the Physics Phase is .05 MWa/m^2. In this paper, activation due to D and D-He3 operation is assumed negligible and the targeted fluence, i.e., the .05 MWa/m^2, is assumed to be attained solely by the D-T operation. The fusion power in this phase is 1100 MW and the average neutron wall loading is .934 MW/m^2. Therefore, the fluence goal corresponds to about 20 full power days (FPD) of operation extended over two calender years.

After the Physics Phase, the Technology Phase starts, using the same hardware, and operates for about eight years at fusion power level of 860 MW and about .73 MW/m^2 average neutron wall loading. The fluence goal for this phase is 1 MWa/m^2, i.e., about 1.37 full power year (FPY), however, the machine is designed to tolerate fluences up to 3 MWa/m^2 (4.11 FPY). This makes ITER the first fusion experiment to achieve such fluence and consequently the first to reach activation levels anticipated for fusion power reactors. From a nucleonics point of view and apart of the different fusion power levels in the two phases, both phases are identical except for the different methods envisaged to protect the first wall (FW). In the Physics Phase 2 cm thick graphite tiles are used and in the Technology Phase the FW will be coated by .05 cm thick tungsten layer. Table 1 lists some of the characteristics of the current ITER design which are relevant to this work.

In this paper, the calculational procedure is presented followed by the radioactivity, decay heat, and the biological dose results. The divertor activation, based on another model, is then presented. Finally the effect of the pulsed operation on the activation is discussed.

Table 1. ITER's Parameters

Major radius (m)	6.00	
Minor radius (m)	2.15	
	Physics	Technology
Fusion power (MW)	1100	860
Wall coating	graphite	tungsten
thickness (cm)	2.	.05
Wall loading (MW/m2)		
Maximum	1.54	1.20
Minimum	0.18	0.14
Average	0.93	0.73
Fluence (MWa/m2)	0.05	1.(3.[a])
Effective full power(days)	<24	500(1500[a])
Number of DT pulses	3456	17000
Flat burn(sec)	250-1000	2300
Effective full power(days)[b]	24.3	1360

a) Design goal.
b) The values used in the calculations and are based on the number of pulses and their burn times.

* Work supported by the U.S. Department of Energy, Office of Fusion Energy, under Contract No. W-31-109-Eng-38.

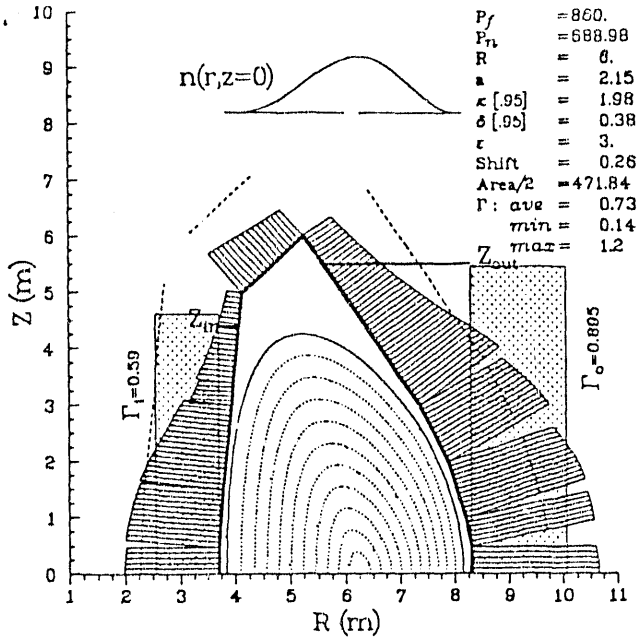

Figure 1. A schematic of the first wall, the neutron wall loading, the source profile, and the inboard and the outboard vertical limits and their average wall loadings.

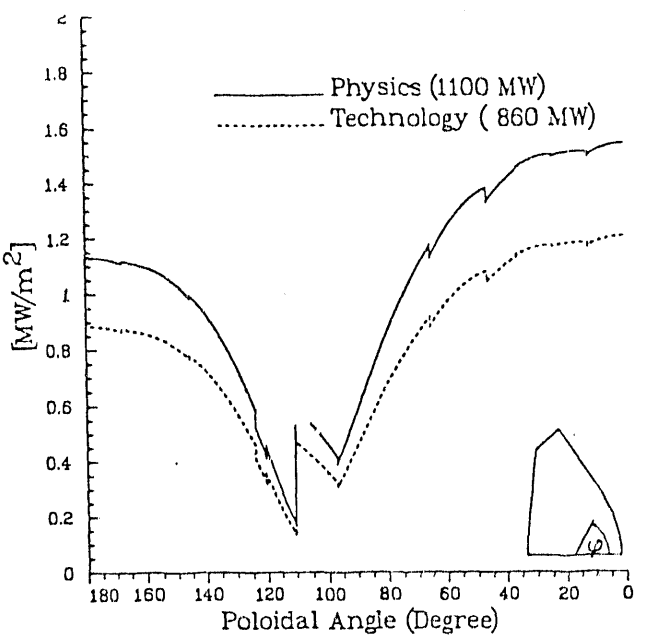

Figure 2 The neutron wall loading poloidal distributions for the two phases of ITER.

CALCULATIONAL PROCEDURE

Unfortunately, there is no reliable multidimensional deterministic transport computer code that is capable of modeling the complicated tokamak geometry accurately and calculating the neutron flux, which is the key input for the activation calculations, authentically. On the other hand, utilizing the neutron flux calculated by 3-D Monte Carlo method in the activation calculations would impregnate its results with the large statistical errors inherent to the calculated Monte Carlo flux. Thus, one-dimensional modeling remains the only available path for the activation calculations, and it is important to realize the limitations of the 1-D modeling and to understand the employed approximations in order to interpret the obtained activation results correctly.

Neutron Wall Loading

Figure 1 shows the contours of the neutron source in ITER, the source distribution at midplane (at top), the first wall boundary, and a schematic of the neutron wall loading in the Technology Phase as calculated by the NEWLIT code[1]. Figure 2 shows the poloidal distributions of neutron wall loadings in the two ITER phases. The large variation of the neutron wall loading is evident and ranges from 165% to 18% of the nominal wall loading (defined as: total 14 MeV neutron power/total first wall surface area ≡ .73 MW/m² for the Technology Phase).

Geometry

Figure 1 suggests that a reasonable 1-D modeling of the reactor, in the transport calculations, could be made using the one-dimensional cylindrical toroidal geometry. In this model, the cylinder axis is the vertical axis of the reactor, the inboard and the outboard blankets/shields are modeled with their midplane compositions, and the neutron source is extended between the midplane plasma boundaries. This allows for the mutual neutronic coupling between the inboard and the outboard blankets/shields as well as the toroidal effect on the calculated neutron flux.

The first obvious assumption in this model is the full coverage of the FW/blanket/shield, i.e., no account is made for the large penetrations in the reactor. The second assumption is the discount of any poloidal (vertical) variations of the neutron wall loading, the neutron source incident angle, and the radial build of the blanket/shield. The model deals with and produces average vertical (poloidal) values representing part of the system rather than localized values that could deviate considerably from the system average. Another assumption is the nucleonic decoupling of that part of the system, modeled in the calculations, from the rest of the system. The larger the modeled part is, the less effect this assumption has. These assumptions, in general, tend to overestimate the radioactivities.

The average values of the neutron wall loadings used in the calculations depend on the vertical extents of the inboard and the outboard blankets and shields. The inboard and the outboard blankets/shields are assumed to extend vertically from z=-4.4 m to z=+4.4 m and from z=-5.5 m to z=+5.5 m, respectively. Within these limits, the inboard receives 18.4% of the neutron power and the outboard receives 73.8% of the neutron power. In the Technology Phase, these neutron power fractions correspond to 126.8 MW for the inboard and 508.4 MW for the outboard. The corresponding average neutron wall loadings are .59 MW/m² on the inboard and .895 MW/m² on the outboard. These powers and neutron wall loadings values should be scaled by 1.28 to obtain the Physics Phase values. In the 1-D cylindrical model, with constant first walls' radii and for the same powers and neutron wall loadings, the inboard/outboard effective vertical heights are 9.2 m and 10.9 m, respectively and are shown schematically in Figure 1. These heights should be used to obtain the total inboard or the total

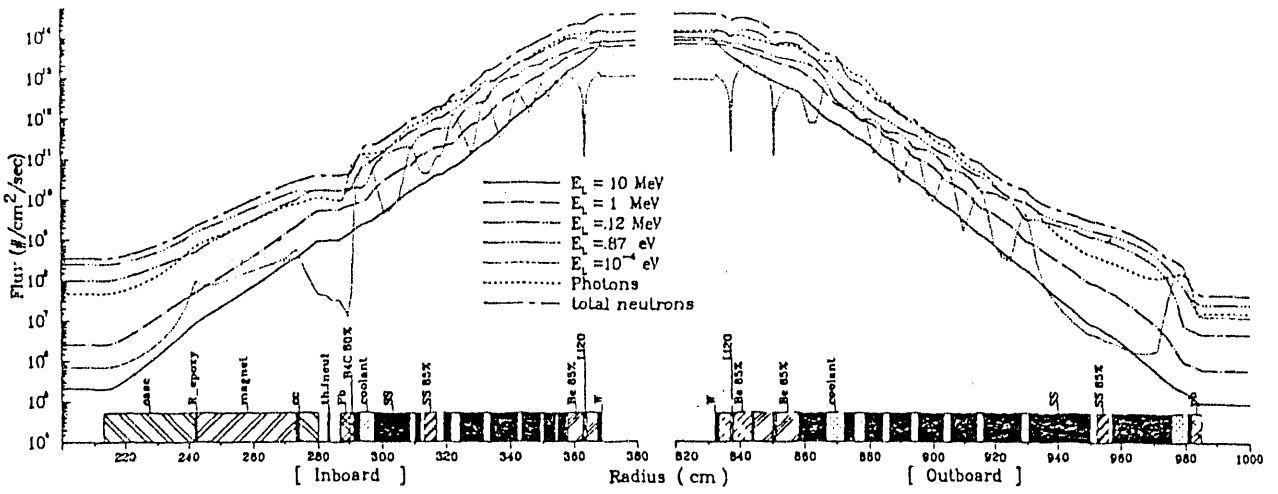

Figure 3 The midplane radial build of ITER and the neutrons and photons fluxes.

outboard value of any response given here as an average per one cm height.

In the transport calculations, the neutron source is assumed uniform over the plasma region leading to different inboard/outboard neutron wall loadings from the ones just mentioned. Therefore, the neutron flux, used in the activation calculations, has been normalized to account for the accurate average neutron wall loadings on the inboard and the outboard first walls.

Computer Codes

The transport calculations have been made with the ONEDANT code[2] with the P3-S8 approximation utilizing the coupled 46-group neutron and 21-group photon cross section library[3] based on VITAMIN-E library[4]. The activation responses are calculated with the RACC code[5] and its associated data libraries RACCDLIB and RACCXLIB which utilize the same group structure.

RADIAL BUILD AND NEUTRON FLUX

The current US blanket and shield design proposed for ITER utilizes the water-cooled solid-breeder blanket concept for tritium breeding and stainless steel (Type 316SS, Annealed) for shielding. Lithium oxide (Li_2O), with 95% Li_6 enrichment is used for tritium breeding and beryllium, with 65% and 85% density factors, is utilized for neutron multiplication as well as for controlling the breeder temperature. The first wall, integrated with the blanket, is 1.5 cm thick water-cooled layers of stainless steel the first layer of which is .5 cm thick and is coated by 2 cm thick carbon tiles in the Physics Phase and .05 cm tungsten in the Technology Phase.

Figure 3 shows a schematic of the midplane radial build-up of ITER together with the neutron and photon fluxes. In this figure, and in order to show the characteristics of these fluxes and the effects of the different materials on them, the 21 photon groups are collapsed into only one group, and the 46 neutron groups are collapsed into 5 major energy groups whose lower energy limits are 10 MeV, 1 MeV, .12 MeV, .87 eV, and 10^{-4} eV.

The inboard blanket has one breeder zone embedded in a 65% dense beryllium zone, and is followed by the bulk shield and the vacuum vessel. To lessen the radiation damage to the magnet, a 1 cm thick 80% dense B_4C layer and 3 cm thick lead layer are placed after the vacuum vessel. The outboard blanket has two breeder zones enclosed also in Be zones. However, the Be density factors in these zones differ, the front one is 85% and the back one is 65%. As in the inboard, the outboard blanket is followed by massive water-cooled steel layers. A 3 cm thick lead layer is added to the back of the vacuum vessel in order to reduce the gamma dose. As seen in Figure 3, the lead layers at the back of the inboard/outboard shields have reduced the photon flux by about one order of magnitude. The effects of Li_6 and B_4C on the lowest neutron energy group and the effect of Be on the intermediate energy groups is also clear.

RESULTS

Radioactivity

Figure 4 shows the average activity per cm height in ITER after the full and continuous operation of the two phases. Also shown in this Figure is the average activation after the first DT pulse in each phase. The pulse burn times assumed for the one pulse results are 600 and 2310 seconds for the Physics Phase and the Technology Phase, respectively. The average radioactivity in ITER amounts to 1.493 MCi/cm at the shutdown of the Physics Phase, and at the end of the Technology Phase it reaches 2.233 MCi/cm. The corresponding values, after one pulse only, are .806 and .783 Mci/cm. The higher value of the first phase (Physics) after one pulse reflects the higher power and consequently, the more generations of the short-lived isotopes. On the other hand, after the full operations of the two phases, the second phase has higher activation level because of its higher fluence which leads to more accumulation of the longer lived isotopes.

Focusing on the Technology Phase, Figure 5 compares the contributions of the different parts of the reactor to the average radioactivity in this phase. The contributions of the outboard zones and the inboard zones to the average radioactivity are 70% to 65% and 30% to 35%, respectively. At shutdown, the Be/Li zones produce about 30% of the average activity, however, this contribution vanishes in few seconds. It is remarkable that

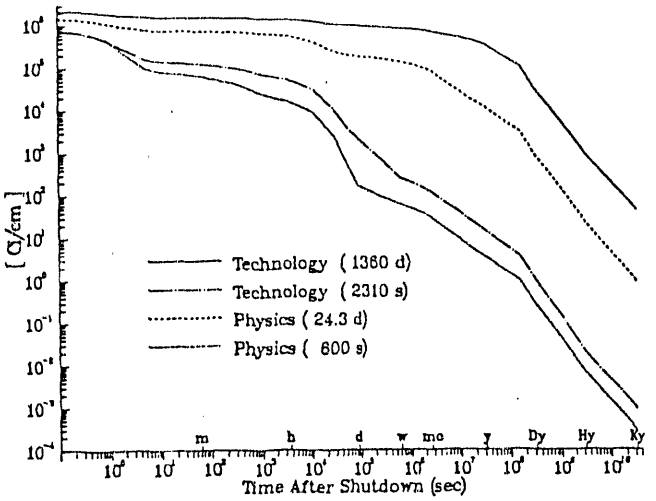

Figure 4 The average activity per cm height after the operation of the two phases, and after one DT pulse in each phase.

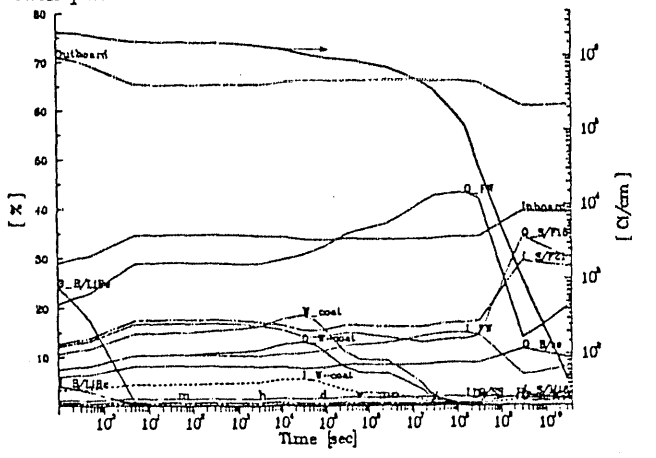

Figure 5 The zonal contributions to the average activity after the Technology Phase operation.

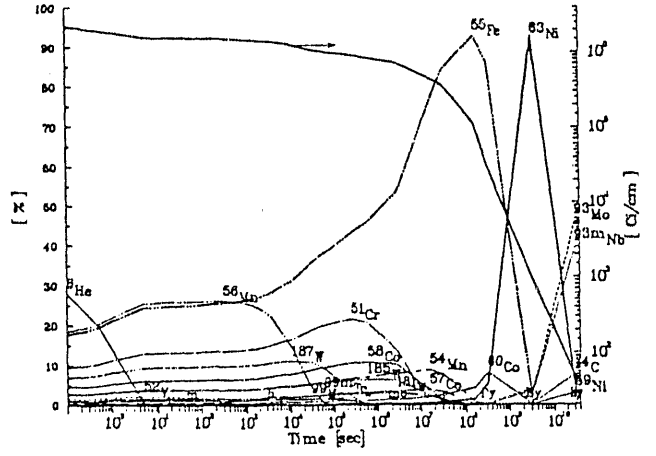

Figure 6 The isotopic contributions to the average activity after the Technology Phase operation.

the .05 cm FW tungsten coating (inboard and outboard) produces more than 10% of the activation of the whole machine for about one day after shutdown. Furthermore, the outboard first wall produces more activity than the entire inboard zones after one day from shutdown and for about 10 years. As expected, the concentration of the radioactivity in the first wall is high. At shutdown, the inboard FW has 8 kCi/cc, and the outboard has 10 kCi/cc. However, the specific radioactivity of the FW coating is even higher; the inboard and outboard FW coatings possess 61 kCi/cc and 63 kCi/cc, respectively, and remain the hottest parts of the machine for about one year.

Figure 6 demonstrates the isotopic contributions to the average activity after the Technology Phase shutdown. The dominant isotopes are: ^{6}He [.8s,^{9}Be(n,α)] at shutdown, ^{56}Mn [2.6 h, ^{9}Be(n,γ)] up to 1 hour, ^{55}Fe [2.68 y, ^{54}Fe(n,γ)] from 1 hour to 10 years, ^{63}Ni [100 y, ^{62}Ni(n,γ)] from 12 years to 100 years, and ^{93}Mo [3500 y, ^{92}Mo(n,γ)] beyond 500 years.

Decay Heat

The time dependence of the decay heat generation rates (DHGR) after the shutdown of both ITER phases and after the first DT shot in the two phase is similar to that of the radioactivities. After the first DT shot, the DHGRs are 8.63 and 8.58 kW/cm for the Technology and the Physics phases, respectively. At the end of the Physics Phase, the DHGR is 15.65 kW/cm compared to 15.57 kW/cm at the end of the Technology Phase.

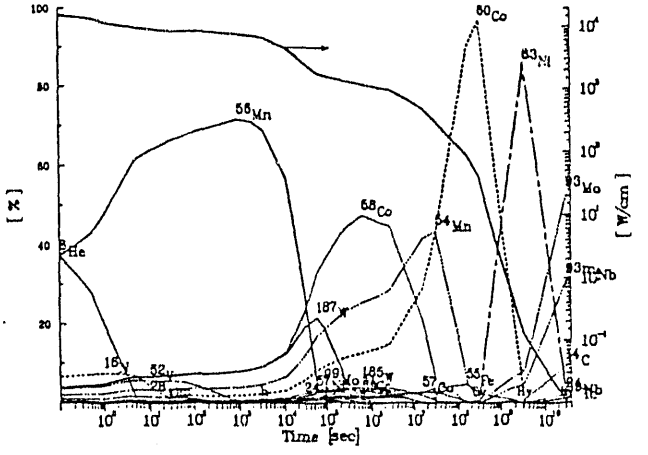

Figure 7 The isotopic contributions to the average afterheat after the Technology Phase operation.

The isotopic contributions to the DHGR, however, is different from that in the radioactivity case. Figure 7 illustrates these contributions after the second phase operation. Here, ^{56}Mn with its 1.69 MeV $< \gamma >$ and .83 MeV $< \beta >$ produces 40% to 70% of the total DHGR for about 4 hours, after which, ^{58}Co [71 d; ^{59}Co(n,2n); 1 MeV $< \gamma >$, EC, β] takes the lead for about two months. After that, ^{54}Mn [312 d; .84 Mev $< \gamma >$] dominates for about 9 months, and then, ^{60}Co [5.3 y; 2.5 MeV $< \gamma >$] followed by ^{63}Ni become the leading contributors to the afterheat.

The integration of the DHGR reveals that there are more than 81 GJ/cm of nuclear radiation stored in the reactor at shutdown and are released over 1000 years with the rate shown in Figure 7. In one week after shutdown, however, only 1 GJ/cm would have been released and is due mainly to ^{56}Mn disintegration. The integration of the DHGR of each isotope provides more indicative measure of the importance of the isotope, since it combines the effects of its concentration (which is function of

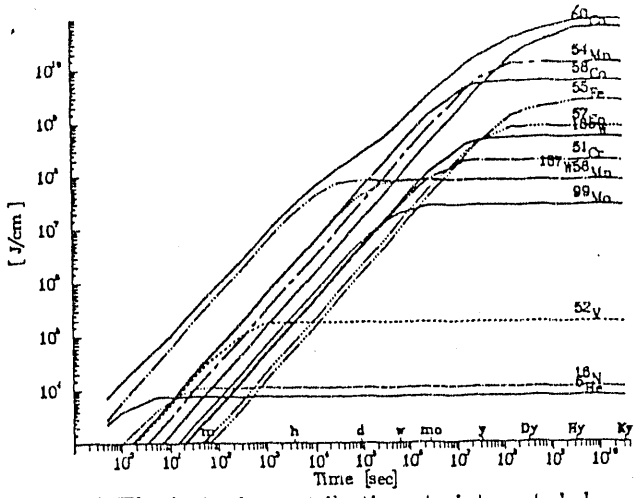

Figure 8 The isotopic contributions to integrated decay heat after the Technology Phase operation.

the cross sections producing it), its disintegration energy, and its half-life. Figure 8 exhibits the integrated DHGRs of the isotopes contributing more than 1% to the total integrated DHGR at any time. With this restriction, the isotopes ^{60}Co, ^{54}Mn, ^{58}Co, ^{55}Fe, and ^{186}W have the largest stored energy.

Dose After Shutdown

The doses to personnel after the full operations of the two ITER phases have been calculated everywhere in the reactor and at different times after shutdown. The neutron fluxes calculated by the ONEDANT transport code are used by the radioactivity code RACC to generate the point-wise 21 groups decay gamma sources at the different times after shutdown. The gamma source, at each time step after shutdown, is then used in the ONEDANT code to calculate the gamma flux and the biological dose rate everywhere in the reactor. In addition to the radial-build shown in Figure 3, a 7 cm thick stainless steel cryostat and a 2 m thick steel reinforced concrete located at radii of 13 and 15.7 m, respectively, are included in the transport and the dose calculations.

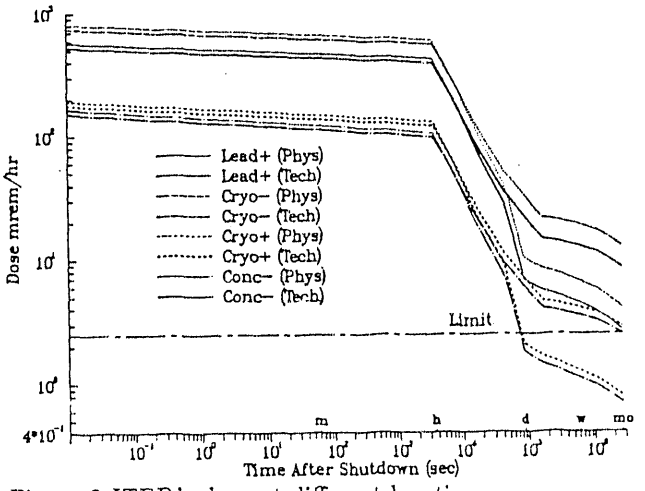

Figure 9 ITER's dose at different locations.

Figure 9 shows the dose rates of the two phases as functions of time after shutdown at: just outside the outboard lead zone (Pb+), inside the cryostat (cryo-), outside the cryostat(cryo+), and just inside the concrete (conc-). The horizontal line in this Figure represents the recommended dose rate limit of 2.5 mrem/hr for a full time worker. It is clear that this limit could be achieved in a reasonable time (1 day) only after the physics phase operation and only in the region between the cryostat and the concrete. Otherwise it would take more than one month to reach that limit.

Divertor Activation

The divertor activation's responses have been calculated using a 1-d cylindrical poloidal model, which is different from the above model. Here, the neutron source is in the center of the cylinder and only the divertor zones are included. In this model, the divertor plate (DP) consists of .2 cm thick pure tungsten, .2 cm thick Nb1Zr, 1 cm thick coolant zone, and .4 cm thick Nb1Zr zone. The volumetric composition of coolant zone is 28.6% Nb1Zr and 71.4% water. The DP is followed by 30 cm vacuum and 60 cm stainless steel shield (80% SS316l, 20% water). The used composition, in wt%, of the Nb1Zr is : Nb balance, .0002 H, .0065 C, .009 N, .0205 O, .099 Si, .95 Zr, .00061 Ta, .000299 W.

The DP is subjected to an average neutron wall loading of about .512 MW/m^2 in the Physics Phase and about .4 MW/m^2 in the Technology Phase. The calculations have been made for 24.3 FPD of operation of the Physics Phase and 1.25 FPY of operation of the Technology Phase. The latter operation time is longer than the expected life-time of the DP. These operation times corresponds to about .027 MWa/m^2 neutron fluence in the Physics Phase, and .5 MWa/m^2 in the Technology Phase.

Figure 10 shows the activity build-up in the four DP's zones as a function of the operation time in the Physics and the Technology Phases. For about 8 hours of continuous operation, the specific activities in the NbZr zones are higher than the W's specific activity. After that, the W's specific activity is several times higher than the NbZr zones' specific activities. It reaches 115 Ci/cc at the end of the Physics Phase, and about 160 Ci/cc at the end of the 1.25 FPY operation in the Technology Phase.

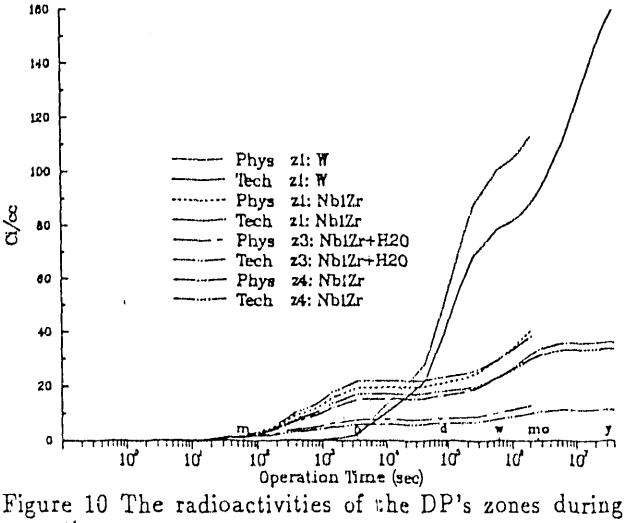

Figure 10 The radioactivities of the DP's zones during operation.

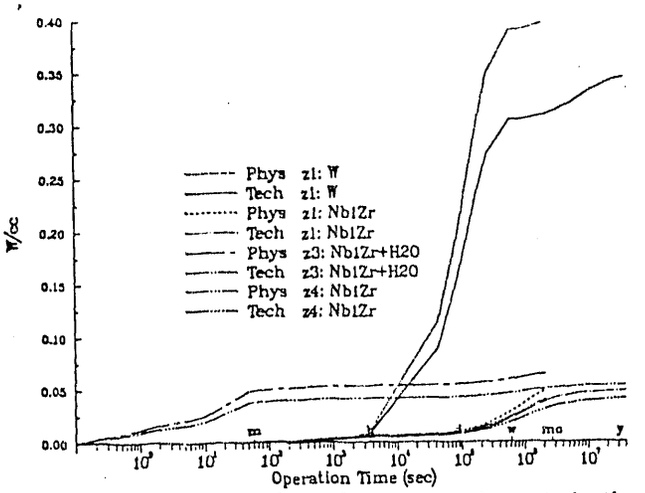

Figure 11 The specific decay heat generation rate in the DP's zones during operation.

Figure 11 shows the specific DHGR's in the DP's zones. In this case also, the activation level in the W is higher than the activation levels in the NbZr zones after a few hours of operation. It is clear in this figure that at the end of the physics phase operation, the DHGRs are larger than the DHGRs at the end of the expected operation time of the DP in the technology phase.

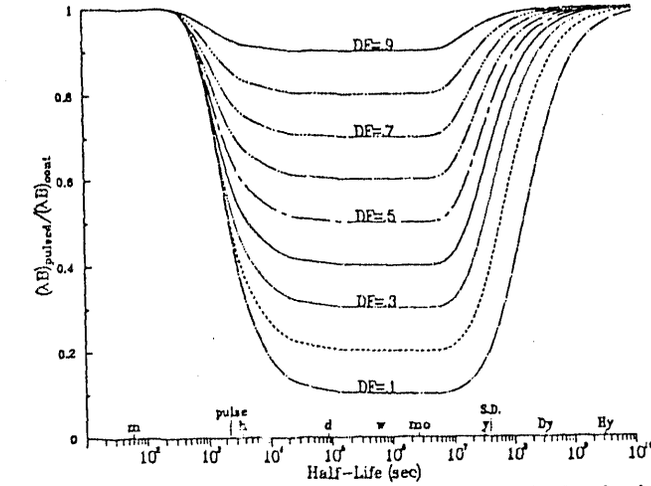

Figure 12 The ratio of the activity at the end of pulsed operation (pulse width=2300 sec) to the activity at the end of continuous operation for different duty factors and as function of the half-life.

EFFECT OF PULSED OPERATION

To understand the effect of pulsed operation on the activation results, consider the simple, but most important, reaction chain $A \xrightarrow{\sigma\phi} B \xrightarrow{\lambda_b} C$. In continuous operation, B reaches its maximum activity at time τ_m, given by $\tau_m = ln(\lambda_b/\sigma\phi)/(\lambda_b - \sigma\phi)$. Usually $\lambda_b > \sigma\phi$ leading to $\tau_m = f * T_b$, where T_b is the half-life of B, and $f = 1.44 * ln(\lambda_b/\sigma\phi)$ and is of small magnitude. In pulsed operation, the activation of B depends on λ_b, the pulse duration T_{on}, and the off time between pulses T_{off}. If $\tau_m << T_{on}$, i.e., short-lived isotope, B reaches it maximum activity (or close to it) at every pulse, and the effect of pulsing is negligible. On the other extreme, when $\tau_m >>$ the effective operation time T_{eff}, i.e., long-lived isotope, the build up of B occurs during each pulse with negligible decay during the off times, and in this case also, the effect of pulsed operation is negligible.

In the case when $T_{on} < \tau_m < T_{eff}$, the decay of B becomes appreciable during the off times. It is found[6], in this case and for the same fluence, that the B's activity at the end of the pulsed operation equals to its activity at the end of the continuous operation multiplied by the duty factor $(= T_{on}/(T_{on} + T_{off}))$. Figure 12 shows the ratio of the pulsed operation to the continuous operation activation for $T_{on} = 2310$ seconds, as function of the half-life time and for different duty factors. For ITER's duty factor, pulses' widths, and for most of the important isotopes, there is a large reduction in the activities as predicted by the continuous operation results. The reduction should be considered as a built-in safety factor when using the continuous operation results.

SUMMARY AND CONCLUSIONS

The activation analysis for the ITER two phases has been made utilizing a one-dimensional cylindrical toroidal model. The analysis shows that at the end of ITER operation, the radioactivity and the afterheat reach 2.23 MCi/cm and 15.57 kW/cm, respectively. The dose calculations show that the present shield configuration is not adequate to provide access to the region outside the cryostat within a reasonable time after the Technology Phase operation. It is shown that for both short-lived and long-lived isotopes, the pulsed operation has negligible effect on the activation results that assume continuous operation. For isotopes whose half-lives are longer than the pulse width and shorter than the effective operation time, the activation results, assumed continuous operation, should be modified by the duty factor.

REFERENCES

1. H. ATTAYA AND M. SAWAN, "NEWLIT - A General Code for Neutron Wall Loading Distribution in Toroidal Reactors," Fusion Technology, 8/1, 608(1985).
2. R. O'DELL et al., "User's Manual for ONEDANT: A Code Package for One-Dimensional, Diffusion accelerated, Neutral Particle Transport," LA-9184-N, Los Alamos National Laboratory (1982).
3. Y. GOHAR, "A coupled 46-Neutron, 21-Photon Multigroup Nuclear Data Library for Fusion Analysis Based on ENDF/B-V," Argonne National Laboratory (to be published).
4. R.W. ROUSSIN et al., "VITAMIN-E: A Coupled 174 Neutron, 38 Gamma Ray Multigroup Cross-Section Library for Deriving Application Dependent Working Libraries for Radiation Transport Calculations," ORNL/RSIC-XX, Oak Ridge National Laboratory (1984).
5. J. JUNG, "Theory and Use of the Radioactivity Code Racc," ANL/FPP/TM-122, Argonne National Laboratory (1979).
6. H. ATTAYA, "The Effect of Pulsed Operation on the Radioactivity," Argonne National Laboratory (to be published).

END

DATE FILMED

02 / 04 / 91